

## استفاده از نانوکامپوزیت مغناطیسی پلی آنیلین/ماگمیت برای حذف سرب از محیط‌های آبی

فاطمه صابر ماهانی\*، لیلی ایران نژاد، نصرت مددی ماهانی

بخش شیمی، دانشگاه پیام نور، صندوق پستی ۱۹۳۹۵-۳۶۹۷، تهران، ایران

تاریخ دریافت: ۲۰ اردیبهشت ۱۳۹۷ تاریخ پذیرش: ۲۸ اردیبهشت ۱۳۹۷

## Using Polyaniline/Maghemite Magnetic Nanocomposite for Removal of Lead from Aqueous Solutions

Fatemeh Sabermahani\*, Leyli Irannejad, Nosrat Madadi Mahani

Department of Chemistry, Payame Noor University, 19395-3697, Tehran, Iran

Received: 10 May 2018

Accepted: 18 May 2018

### چکیده

نانوکامپوزیت مغناطیسی پلی آنیلین/ماگمیت (PANI/ $\gamma$ -Fe<sub>2</sub>O<sub>3</sub> MNC) به عنوان یک واکنشگر فعال برای حذف سرب از محیط‌های آبی استفاده شد. روش هم‌رسوبی شیمیایی برای تهیه نانوذرات ماگمیت بکار رفت و به دنبال آن نانوکامپوزیت مغناطیسی از طریق پلیمریزاسیون آنیلین تهیه گردید. سطح آن توسط IR FT-IR مشخص گردید. راندمان این نانوکامپوزیت برای حذف سرب به روش ناپیوسته بررسی شد. نتایج نشان داد که شرایط بهینه برای حذف سرب در pH=6، مقدار جاذب 0.4/گرم و زمان تماس 90 دقیقه رخ می‌دهد. سینتیک جذب مطالعه شد و با معادله سرعت مرتبه دوم مطابقت داشت. ایزوترم‌های جذب بررسی گردیدند. مدل ایزوترم جذبی فروندلیچ تطابق بیشتری نسبت به لانگمویر داشت. مطالعات ترمودینامیکی دلالت بر خودبخودی و گرماگیر بودن فرایند جذب سرب داشت.

### واژه‌های کلیدی

جذب سطحی؛ پولیمر هادی؛ سرب؛ نانوکامپوزیت؛ حذف.

### Abstract

Polyaniline/maghemite magnetic nanocomposite (PANI/ $\gamma$ -Fe<sub>2</sub>O<sub>3</sub> MNC) was used as active agents for removal of lead ions from aqueous media. Chemical co-precipitation method was used to prepare the maghemite nanoparticles. Subsequently, the MNC was synthesized through polymerization of aniline. It was characterized by FT-IR. The efficiency of this MNC was estimated for Pb (II) removal by using batch method. The results showed that optimum conditions for lead removal were found to be at pH of 6, adsorbent dosage of 0.04 g and equilibrium contact time of 90 min. The kinetic of adsorption system have been studied based on the assumption of a pseudo-second order rate law. The adsorption isotherms were examined. The Freundlich adsorption isotherm model was found to represent the equilibrium adsorption isotherm better than Langmuir isotherm. The thermodynamic studies indicated that the adsorption was spontaneous and endothermic process for lead.

### Keywords

Adsorption; Conducting Polymer; Lead; Nanocomposite; Removal.

### 1. INTRODUCTION

The discharge of heavy metal pollutants into the environment from sewage, industrial and mining waste effluents is a serious problem due to its impact on human health and natural environment. These numerous metal ions such as Zn<sup>2+</sup>, Cr<sup>3+</sup>, Cd<sup>2+</sup>, Pb<sup>2+</sup>, Mn<sup>2+</sup>, and Hg<sup>+</sup> are non-biodegradable, highly toxic and probably have a carcinogenic effect [1,2]. Since they come into the food chain, due to their high solubility in the aqueous phases, high concentration of heavy metals may

accumulate in the human organs. Lead contamination is known as one of the most pervasive and elusive environmental health threats, as considered by the fact that exposure lead(II) has been associated with death and disease in humans, birds, and animals. The lead (II) ions concentration is approximately in the range of 200–500 mg dm<sup>-3</sup> in industrial wastewaters, according to water quality standards; this value is very high and must be reduced to a value of 0.10–0.05 mg dm<sup>-3</sup> [3].

\*Corresponding Author: fatemehsaber2003@yahoo.com

Chemical precipitation, membrane filtration, electrochemical method, flotation, coagulation–flocculation, membrane process, ion exchange, and adsorption are some of the conventional methods that have been used for removal of heavy metals from water and wastewater [4,5]. In spite of the fact that many remediation technologies exist, most of them can be ineffective at low metal concentrations (1–20 mg/L). Also, sometimes these removal procedures involve a high cost for their implementation [6]. In the last few years, several methods have been applied in this area. The literatures suggested the use of various synthetic and natural adsorbents for removal of heavy metals from waste water [7-11], but, most of them are not selective, have long contact time, and some of them low capacity for adsorption. The MNPs most used to this end are magnetite ( $\text{Fe}_3\text{O}_4$ ) and maghemite ( $\gamma\text{-Fe}_2\text{O}_3$ ), due to their high saturation magnetization, low toxicity and biological compatibility [12,13]. However, the use of pure iron oxide particles has as a drawback the tendency of these MNPs to form agglomerates, and so it is usually necessary to modify the surface of the particles to prevent the self-aggregation [14]. Furthermore, in this process one can attach to the MNP functional groups that can selectively interact with the target element [15,16]. Some of the materials that have been reported to modify the surface of the MNPs are mesoporous silica [17], polyethylenimine (PEI) [18], amino-modified silica [19], streptavidin [20], thiol functionalized PAMAM dendron [21] and carboxyl groups [22]. Other materials that have attracted attention are conducting polymers such as polypyrrole and polyaniline (Pani), due to their low cost of synthesis, biocompatibility, special electrical and optical properties, and excellent environmental stability [23].

In this work, we have synthesized the maghemite MNPs by co-precipitation method, and later we used them to prepare the PANI/ $\gamma\text{-Fe}_2\text{O}_3$  MNC after the polymerization of aniline. Nanocomposite was prepared by in situ oxidative polymerization. The adsorption performance of the PANI/ $\gamma\text{-Fe}_2\text{O}_3$  MNC for the removal of Pb(II) from aqueous solution was evaluated. The kinetic, thermodynamic and isotherm of the Pb(II) adsorption onto the nanocomposite have also been investigated.

## 2. EXPERIMENTAL

### 2.1. Apparatus and Reagents

An atomic absorption spectrometer model Sens AA (Dandenong, Victoria, Australia) equipped with deuterium lamp background corrector was used for determination of Pb in air-acetylene flame. A mechanical shaker KS 130 basic (Deutschland, Germany) having speed control and

timer was used for preparation of the sorbent. A 691 Metrohm pH meter (Herisau, Switzerland) was employed for pH measurements.

Iron(II) chloride tetrahydrate ( $\text{FeCl}_2 \cdot 4\text{H}_2\text{O}$ ), ammonium persulfate (APS), sodium dodecyl sulfate (SDS), Iron(III) chloride hexahydrate ( $\text{FeCl}_3 \cdot 6\text{H}_2\text{O}$ ), aniline, ammonium hydroxide ( $\text{NH}_4\text{OH}$ ) and hydrochloric acid (HCl) were obtained from Merck (Darmstadt, Germany). All the reagents were used without further purification, except aniline which was distilled prior to use. The stock solution of lead (II) ions used in this work was prepared by dissolving an accurate quantity of  $\text{Pb}(\text{NO}_3)_2$  99.99% (Merck, Darmstadt, Germany).

### 2.2. Synthesis of $\gamma\text{-Fe}_2\text{O}_3$ MNPs

The  $\gamma\text{-Fe}_2\text{O}_3$  MNPs were obtained by a chemical co-precipitation method [24]. Firstly, 25 mL of ( $\text{FeCl}_3 \cdot 6\text{H}_2\text{O}$ ), (2M) was mixed with 25 mL of ( $\text{FeCl}_2 \cdot 4\text{H}_2\text{O}$ ), (1M) solution in a 250 mL round – bottom flask and stirred for 10 min. Then, 125 mL of an aqueous solution of ( $\text{NH}_4\text{OH}$ ) (50% vol) was added and the solution was again stirred for 2 h. After this, the MNPs that had been formed were decanted with a magnet and washed four successive times with deionized water. The MNPs were finally dried at 60 °C in an oven for 48 h. The FT-IR spectrum of  $\text{Fe}_2\text{O}_3$  MNPs is given in Fig. 1.

### 2.3. Preparation of PANI/ $\gamma\text{-Fe}_2\text{O}_3$ MNC

The PANI/ $\gamma\text{-Fe}_2\text{O}_3$  MNC was obtained by in situ chemical polymerization. Initially, 0.3 g of MNPs was mixed in 100 mL of hydrochloric acid 0.1 M in a round bottom flask, and was stirred for 60 min. Then, 5 mL of freshly distilled aniline was slowly added and sonicated for 15 min to obtain a homogenous dispersion. Afterwards, 50 mL of the solution of APS (0.5 M) was added drop-wise to initiate the polymerization process. The reaction was allowed to continue for 4 h at room temperature, under continuous stirring. After a dark colloidal suspension was obtained, greenish black precipitate was washed thoroughly with double distilled water and ethanol to remove the traces of reactants and polyaniline oligomers until the filtrate become transparent. The prepared nanocomposite was dried at 80 °C and stored in desiccator for further experiments.

### 2.4. Characterization method

The  $\gamma\text{-Fe}_2\text{O}_3$  MNPs and PANI/ $\gamma\text{-Fe}_2\text{O}_3$  MNCs were characterized by FT-IR spectroscopy. Comparison of the FT-IR spectrum of  $\gamma\text{-Fe}_2\text{O}_3$  MNPs with PANI/ $\gamma\text{-Fe}_2\text{O}_3$  MNC (Fig. 2), showed many new peaks in the spectrum. With respect to Fig. 2, the peaks at 1582 and 1507  $\text{cm}^{-1}$  are corresponding to quinone and benzene slightly shifted ring-stretching deformations of PAN are

also detected in the nanocomposite. The band at  $1301\text{ cm}^{-1}$  belongs to the C-N stretching of a secondary aromatic amine strengthened by protonation of PAN. All bands in nanocomposites are slightly shifted, which indicates that there is some interaction between PANI and the  $\gamma\text{-Fe}_2\text{O}_3$  MNPs.

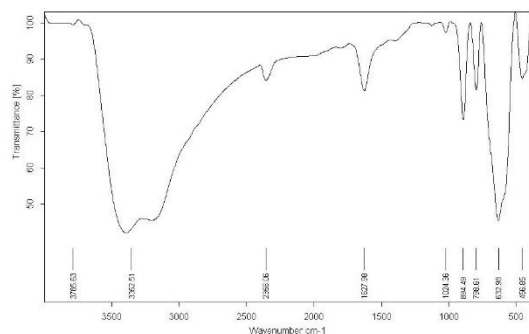


Fig. 1. FT-IR spectrum of  $\text{Fe}_2\text{O}_3$  MNPs.

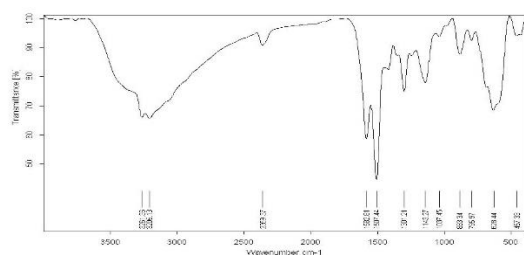


Fig. 2. FT-IR spectrum of PANI/ $\gamma\text{-Fe}_2\text{O}_3$  MNC.

#### 2.4. Adsorption procedure

All adsorption experiments were performed by a batch operation. In order to remove lead from aqueous phase, 10 mL of solution 30 ppm with pH 6 was added to the conical flasks containing desired adsorbent at room temperature. Then, the flasks were placed on a shaker for a given period of time at 250 rpm. The adsorbent was separated by use of a magnet and the supernatant was collected. The final metal concentration was determined by using FAAS.

The percent of removed lead ions (R%), and the amount of lead adsorbed ( $q_e$ ) by the adsorbent was calculated by the following equations:

$$R\% = (C_0 - C_e) / C_0 \quad (1)$$

$$q_e = V(C_0 - C_e) / M \quad (2)$$

where  $q_e$  is the amount adsorbed per gram of the adsorbent,  $C_0$  is initial concentration and  $C_e$  is the equilibrium concentration of the lead ions (mg/L) that is obtained from calibration curve of lead,  $V$  is volume of solution (L) and  $M$  is the mass of the adsorbent (g).

### 3. RESULTS AND DISCUSSION

#### 3.1. Effect of solution pH

The pH of the solution is one of the main parameters that can have an impact on the

adsorption process. A study was carried out of how the pH of the solution would affect the capacity on the MNCs surface to adsorb Pb (II). As can be seen from Fig. 3, removal rate increased with increasing the value of pH. The low adsorption capacity that MNC exhibits at low pH values may be due to the fact that under those conditions the PANI chains are highly protonated, resulting in a cationic repulsion of the Pb (II) ions. As the pH increases, it can be observed that the adsorption capacity also increases, reaching a maximum value of 69% at a pH=6. Then, all subsequent ion removal experiments were performed at pH 6.0.

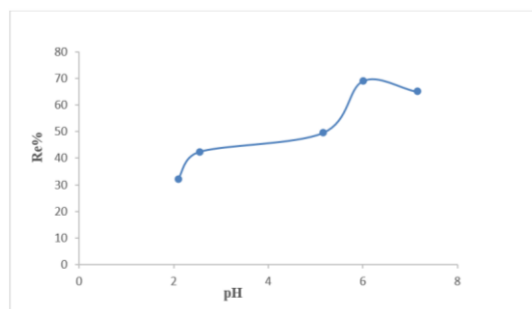


Fig. 3. Effect of pH on the adsorption of lead.

#### 3.2. Effect of interaction time

A second important parameter determining whether or not the use of a given adsorbent is feasible for a particular task is the time it requires to reach the maximum capacity for capturing of analyte. It can be observed that the adsorption capacity increases with the increase in the interaction time. In fact, it took only 10 min for the PANI/ $\gamma\text{-Fe}_2\text{O}_3$  MNCs to capture 55.8% of the Pb (II) present in the solution (Fig. 4). The adsorption equilibrium, which corresponds to a level of removal 86.3%, reached in 90 min. This time was selected for further studies.

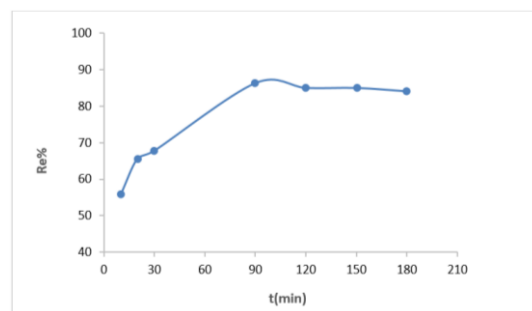


Fig. 4. Effect of the contact time on the adsorption of lead.

#### 3.3. Effect of adsorbent dosage

The removal percentage of lead was studied by varying the adsorbent (PANI/ $\gamma\text{-Fe}_2\text{O}_3$  MNC) dose between 10 and 60 mg at lead ions concentration of 30 ppm. The results showed, the removal

efficiency increases by increasing the dose of adsorbent. This is due to the fact that greater surface area and more adsorption sites create by increasing adsorbent doses. The Pb<sup>2+</sup> removal efficiency reaches to plateau level at high amount of adsorbent dosage. 40 mg was selected for more experiments.

### 3.4. Effect of initial concentration and adsorption isotherms

Naturally, the capacity of adsorption of lead by the (PANI/γ-Fe<sub>2</sub>O<sub>3</sub> MNC) is dependent on the initial metal concentration in the solution. The effect of initial concentration on the adsorption of lead (II) ions by proposed sorbent was investigated with varying solution concentrations (10, 20, 30, 40, 50, 60 and 70 mg/L). With increasing concentration of the solution, q<sub>e</sub> increased, while R% decreased. At low initial solution concentration, the surface area and the availability of adsorption sites were relatively high, and the metals ions were easily adsorbed and removed. At high initial solution concentration, the total available sites are limited, thus resulting in a decrease in percentage removal of the ions. The increased q<sub>e</sub> at high initial concentration can be attributed to enhanced driving force.

Langmuir and Freundlich isotherms have been used to describe observed adsorption phenomena on the adsorbent. The sorption data have been analyzed according to the linear form of the Langmuir isotherm, as represented in Eq. (3)

$$C_e/q_e = (1/Q_m b) + (1/Q_m) C_e \quad (3)$$

b is Langmuir constant which is a measure of energy of adsorption and Q<sub>m</sub> is adsorption capacity expressed in mg/g.

The Freundlich equation predicts that the concentration of metal ions on the adsorbent will increase as long as there is an increase in the metal ion concentration in liquid, as represented in Eq. (4)

$$q_e = K_f C_e^{1/n} \quad (4)$$

where 1/n and K<sub>f</sub> are the constants related to adsorption capacity, and q<sub>e</sub> is the weight adsorbed per unit weight of adsorbent. Taking logs gives Eq. (5).

$$\log q_e = \log K_f + 1/n \log C_e \quad (5)$$

To compare the obtained results with other adsorbents, the Freundlich and Langmuir constants should be determined from Langmuir and Freundlich isotherms. As can be seen from the

Figs. 5 and 6, Freundlich model best fit the equilibrium isotherm data for the lead. The values of constants obtained from intercepted and slope of plots and values of calculated according to Eqs. (3) and (5) are given in Table 1.

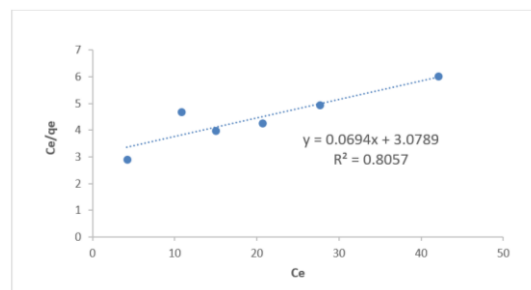


Fig. 5. Langmuir isotherms for adsorption of Pb.

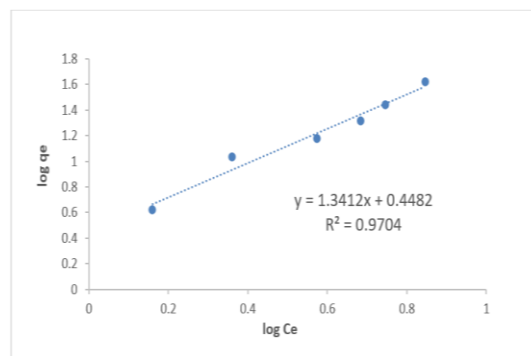


Fig. 6. Freundlich isotherms for adsorption of Pb.

### 3.5. Adsorption kinetics

To better description behavior of the sorbent and possible controlling mechanism, the kinetics experimental data were examined with pseudo-first-order and Pseudo-second order model.

The integral form of Lagergren equation is:

$$\log(q_e - q_t) = \log q_e - (k_1/2.303)t \quad (6)$$

The pseudo-second-order equation is:

$$(t/q_t) = (1/k_2 \cdot q_e^2) + t/q_e \quad (7)$$

where q<sub>t</sub> is the amount of solute adsorbed at 't' time (mg/g), q<sub>e</sub> is the amount of lead adsorbed at equilibrium (mg/g), t is the contact time (min) and k<sub>1</sub> is the adsorption equilibrium rate constant of pseudo-first-order reaction (min<sup>-1</sup>) and k<sub>2</sub> is the rate constant of pseudo-second-order adsorption (g mg<sup>-1</sup> min<sup>-1</sup>). The slope and intercept of plot of log (q<sub>e</sub> - q<sub>t</sub>) against time were used to determine the first-order rate constant k<sub>1</sub>. The calculated values of R<sup>2</sup>, q<sub>e,cal</sub> and q<sub>e,exp</sub> were presented in Table 2.

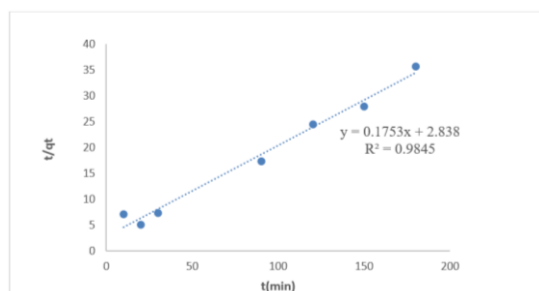
Table 1. Langmuir and Freundlich isotherm constants for lead.

Element	Langmuir isotherm			Freundlich isotherm		
	Q(mg.g <sup>-1</sup> )	b(L. mg <sup>-1</sup> )	R <sup>2</sup>	K <sub>f</sub>	1/n	R <sup>2</sup>
Pb	14.41	0.022	0.80	2.8	1.34	0.97

**Table 2.** Adsorption kinetic constants for lead.

Concentration (mg g <sup>-1</sup> )	First order kinetic model (mg/L)				Second order kinetic model		
	$q_{e,exp}$ (mg g <sup>-1</sup> )	$k_1$ (1/min)	$q_{e,cal}$ (mg g <sup>-1</sup> )	$R^2$	$k_2$ (1/min)	$q_{e,cal}$	$R^2$
30	5.36	0.010	1.912	0.447	0.0108	5.70	0.984

It was observed that correlation coefficient ( $R^2$ ) was low and experimental data are not fitted well for pseudo-first-order reaction. Hence, the adsorption mechanism cannot be well described by pseudo-first-order kinetics. The pseudo-second order rate constant  $k_2$  was calculated from the slope and intercept of the plot  $t/q_t$  against time (Fig. 7). The  $q_{e,cal}$  was very close to  $q_{e,exp}$  value and correlation coefficient was high (Table 2). In the view of these results, it can be concluded that the pseudo-second order model provides a good correlation for adsorption of lead on to the sorbent.

**Fig. 7.** Pseudo-second order kinetic plot for adsorption of lead.

### 3.6. Adsorption thermodynamics

Study of the temperature dependence of adsorption gave valuable knowledge about the enthalpy and entropy changes during adsorption. The removal of lead (II) ions onto the new sorbent was examined at 300, 303, 308, and 313 K. Adsorption ability increased with increasing temperature, illustrating that adsorption of lead onto the sorbent is endothermic process. The apparent equilibrium constant ( $K_c$ ) of the sorption is defined as:

$$K_c = (C_0 - C_e) / C_e \quad (8)$$

where  $C_e$  is the equilibrium concentration. The  $K_c$  value is used in the following equation to determine the Gibbs free energy ( $\Delta G^0$ ) of sorption.

$$\Delta G^0 = -RT \ln K_c \quad (9)$$

$$\Delta G = \Delta S^0 T - \Delta H^0 \quad (10)$$

$R$  the universal gas constant ( $8.314 \text{ J mol}^{-1} \text{ K}^{-1}$ ) and  $T$  is the absolute temperature (K).

The enthalpy ( $\Delta H^0$ ) and entropy ( $\Delta S^0$ ) can be obtained from the slope and intercept of van 't Hoff equation of  $\Delta G^0$  versus  $T$  (Table 3).

The negative values of  $\Delta G^0$  confirm the spontaneous nature of sorption with high performance of metal ions on the sorbent.

**Table 3.** Thermodynamic Parameters for adsorption of lead.

Temperature (K)	$\Delta G^0$ (J mol <sup>-1</sup> )	$\Delta S^0$ (J mol <sup>-1</sup> K <sup>-1</sup> )	$\Delta H^0$ (kJ mol <sup>-1</sup> )
300	-282.368	405.79	120.92
303	-2231.52		
308	-5079.26		
313	-5428.20		

## 4. CONCLUSION

In this study, Polyaniline/maghemite magnetic nanocomposite (PANI/ $\gamma$ -Fe<sub>2</sub>O<sub>3</sub> MNC) was successfully prepared and applied as adsorbent for the removal of Pb from aqueous solutions. It was observed that the equilibrium was achieved within 90 min. The experimental data showed good fit to the Freundlich isotherm. The coefficient of variation ( $R^2$ ) showed experimental data was better described by pseudo second-order model. The endothermic and spontaneous nature of the adsorption was confirmed by thermodynamic studies.

## ACKNOWLEDGMENTS

This work was supported by the Payame Noor University of Kerman. The authors would like to express their appreciations to department of chemistry this university for providing research facilities.

## REFERENCES

- [1] B. Rahmanian, M. Pakizeh, S.A.A. Mansoori and R. Abedini, Application of experimental design approach and artificial neural network (ANN) for the determination of potential micellar-enhanced ultrafiltration process, *J. Hazard.Mater.* 187 (2011) 67-74.
- [2] B. Rahmanian, M. Pakizeh and A. Maskooki, Micellar-enhanced ultrafiltration of zinc in synthetic wastewater using spiral-wound membrane, *J. Hazard.Mater.* 184 (2010) 261-267.
- [3] H. Uzun, Y.K. Bayhan, Y. Kaya, A. Cakici and O.F. Algur, Biosorption of lead(II) from aqueous solution by cone biomass of *Pinus sylvestris*, *Desalination* 154 (2003) 233-238.

- [4] Y. Kong, J. Wei, Z. Wang, T. Sun, C. Yao and Z. Chen, Heavy metals removal from solution by polyaniline/palygorskite composite, *J. Appl. Polym. Sci.* 122 (2011) 2054-2059.
- [5] M. Ghorbani and H. Eisazadeh, Fixed bed column study for Zn, Cu, Fe and Mn removal from wastewater using nanometer size polypyrrole coated on rice husk ash, *Synthetic Met.* 162 (2012) 1429-1433.
- [6] G. Zhao, X. Wu, X. Tan and X. Wang, Sorption of heavy metal ions from aqueous solutions: a review, *Open Colloid Sci. J.* 4 (2011) 19-31.
- [7] F. Fu and Q. Wang, Removal of heavy metal ions from wastewaters: a review, *J. Environ. Manage.* 92 (2011) 407-418.
- [8] M. Ghorbani, M.S. Lashkenari and H. Eisazadeh, Application of polyaniline nanocomposite coated on rice husk ash for removal of Hg(II) from aqueous media, *Synth.Met.* 161 (2011) 1430-1433.
- [9] O.S. Amuda, A.A. Giwa and I.A. Bello, Removal of heavy metal from industrial wastewater using modified activated coconut shell carbon, *Biochem. Eng. J.* 36 (2007) 174-181.
- [10] M.J. Ayotamuno, R.N. Okparanma, S.O.T. Ogaji and S.D. Probert, Chromium removal from flocculation effluent of liquid-phase oil-based drill-cuttings using powdered activated carbon, *Appl. Energ.* 84 (2007) 1002-1011.
- [11] A.K. Bhattacharya, T.K. Naiya, S.N. Mandal and S.K. Das, Adsorption, kinetics and equilibrium studies on removal of Cr(VI) from aqueous solutions using different low-cost adsorbents, *Chem.Eng. J.* 137 (2008) 529-541.
- [12] M. Koroki, S. Saito, H. Hashimoto, T. Yamada and M. Aoyama, Removal of Cr(VI) from aqueous solutions by the culm of bamboo grass treated with concentrated sulfuric acid, *Environ. Chem. Lett.* 8 (2010) 59-61.
- [13] C.M. Monteiro, P.M.L. Castro and F.X. Malcata, Capacity of simultaneous removal of zinc and cadmium from contaminated media, by two microalgae isolated from a polluted site, *Environ. Chem. Lett.* 9 (2011) 511-517.
- [14] A.M.G.C. Dias, A. Hussain, A.S. Marcos and A.C.A. Roque, A biotechnological perspective on the application of iron oxide magnetic colloids modified with polysaccharides, *Biotechnol. Adv.* 29 (2011) 142-155.
- [15] S. Laurent et al., Magnetic Iron Oxide Nanoparticles: Synthesis, Stabilization, Vectorization, Physicochemical Characterizations, and Biological Applications, *Chem. Rev.* 108 (2008) 2064-2110.
- [16] N.T.K. Thanh and L.A.W. Green, Functionalisation of nanoparticles for biomedical applications, *Nano Today* 5 (2010) 213-230.
- [17] C.H. Yu, W. Oduro, K. Tam and E.S.C. Tsang, Some Applications of Nanoparticles, in: A.B. John (Ed.), *Handbook of Metal Physics*, Elsevier, 5 (2008) 365-380.
- [18] X. Li, J. Zhang, H. Gu, *Langmuir* 27 (2011) 6099-6106.
- [19] C.-L. Chiang, C.-S. Sung, T.F. Wu, C.Y. Chen and C.Y. Hsu, Application of superparamagnetic nanoparticles in purification of plasmid DNA from bacterial cells, *J. Chromatogr. B* 822 (2005) 54-60.
- [20] P. Ashtari, X. He, K. Wang and P. Gong, An efficient method for recovery of target ssDNA based on amino-modified silica-coated magnetic nanoparticles, *Talanta* 67 (2005) 548-554.
- [21] T. Lund-Olesen, M. Dufva and M.F. Hansen, Capture of DNA in microfluidic channel using magnetic beads: Increasing capture efficiency with integrated microfluidic mixer, *J. Magn. Magn. Mater.* 311 (2007) 396-400.
- [22] T. Tanaka et al., Characterization of magnetic nanoparticles modified with thiol functionalized PAMAM dendron for DNA recovery, *J. Colloid Interface Sci.* 377 (2012) 469-475.
- [23] Z. Shan et al., Bacteria capture, lysate clearance, and plasmid DNA extraction using pH-sensitive multifunctional magnetic nanoparticles, *Biochem.* 398 (2010) 120-122.
- [24] S. Bhadra, D. Khastgir, N.K. Singha and J.H. Lee, Bacteria capture, lysate clearance, and plasmid DNA extraction using pH-sensitive multifunctional magnetic nanoparticles, *Prog. Polym. Sci.* 34 (2009) 783-810.
- [25] J. Apesteguy and S. Jacobo, Synthesis of a soluble polyaniline-ferrite composite: magnetic and electric properties, *J. Mater. Sci.* 42 (2007) 7062-7068.